ELSEVIER

Fuel 81 (2002) 413–421

FUEL

www.fuelfirst.com

Contribution of organic and mineral compounds to the formation of solid deposits inside petroleum wells ☆

A. Cosultchi[a,b,*], E. Garciafigueroa[b,c], B. Mar[b], A. García-Bórquez[c], V.H. Lara[d], P. Bosch[d]

[a]*Department of Metallurgical Engineering, ESIQIE-IPN, Mexico City, Mexico*
[b]*Instituto Mexicano del Petroleo, 152, Eje Central "L. Cardenas", 07730 Mexico City, Mexico*
[c]*ESFM-IPN, UPALM, Ed. 9, 07738 Mexico City, Mexico*
[d]*UAM-I, Av. Michoacan y Purisima, Iztapalapa, 09340 Mexico City, Mexico*

Received 24 May 2001; revised 1 October 2001; accepted 1 October 2001; available online 13 November 2001

Abstract

Deposit samples collected from three Mexican wells, their asphaltene and residue fractions as well as the sediment and asphaltene fractions separated from the corresponding crude oils were characterized. An appreciable amount of minerals such as $CaCO_3$, $BaSO_4$, NaCl, quartz and iron compounds were detected in the deposit compositions. Additionally, aromatic factors and structural parameters such as interlayer distance and crystallite diameters were calculated from the (γ) and (002) characteristic bands from the X-ray diffractograms of the deposits, deposit-asphaltene, oil-asphaltenes as well as oil-sediments. FTIR, elemental analysis and thermal techniques were also used to elucidate the sample compositions. The stages of the deposit formation inside petroleum wells include steel surface corrosion products formed in situ by the presence of brine and sulfur bearing compounds and adsorption or chemisorption of organic compounds on the modified tubing steel surface and mineral pores. Moreover, the high amount of vanadium and nickel indicates a time-dependent process of accumulation of some organometallic compounds independent of the oil-asphaltene amount.

Keywords: Petroleum deposits; Asphaltene; Oil-sediments; XRD; FTIR; TGA–DTG

1. Introduction

The flow of petroleum out of the reservoir is often restricted by the presence of solid or semi-solid material adhered on the internal wall of the production tubing. Consequently, the internal diameter of the tubing diminishes and modifies the flow pattern, and therefore, the crude oil extracted volume shrinks. Even though the characterization of solid deposits has been performed occasionally only [1,2], the petroleum well blocking was attributed to asphaltene flocculation and precipitation [3]. However, as shown recently, the asphaltenes induced by flow pressure reduction inside the well were considered different from those prepared by solvent precipitation [4]. Additionally, the concurrence of organic compounds as well as minerals point out a different mechanism of formation of such deposits. Interactions between organic compounds and mineral or metals have been overlooked in petroleum engineering studies, although they have been examined in reservoir researches, soil science and catalytic chemistry. For example, during the diagenesis and maturation of sedimentary organic matter process, the organic material is trapped in the mineral micropores. Indeed, the irreversibility of adsorption of organic compounds on clay minerals and their catalytic effect with polymerization or condensation of the organic material are well documented [5]. Moreover, iron-rich clays concentrate a higher amount of organic material than other types of clays. Additionally, iron compounds, as ferric ion (Fe^{3+}), contribute to increase the amount of material precipitated from crude oil, and especially polar compounds [6]. The adsorption of asphaltene on dolomite mineral was reported as a dynamic and continuous process by which the amount of adsorbed material increases as a function of time of contact [7].

In this work, a characterization sequence was applied in order to acquire the elemental, crystalline and organic composition as well as the thermal behavior of three deposits and the solid fractions separated from their respective crude oils.

In order to characterize heavy carbonaceous material, the TGA/DTG technique was applied additionally to the

* Corresponding author. Address: Instituto Mexicano del Petroleo, 152, Eje Central "L. Cardenas", 07730 Mexico City, Mexico. Tel.: +52-5-3337013.
E-mail address: acosul@imp.mx (A. Cosultchi).

☆ Published first on the web via Fuelfirst.com—http://www.fuelfirst.com

0016-2361/02/$ - see front matter
PII: S0016-2361(01)00187-9

Table 1
Characteristics of the petroleum wells and crude oils

Characteristics	K101 well	CH2 well	T101 well
Well origin	Marine	Continental	Marine
Production interval depth (m)	4580–4600	5180–5193 5145–5265	4290–4300
API gravity 60/60 °F	29.5	32.86	32
Asphaltene (wt%)	3.1	2.5	8.5

conventional separation procedures with solvents [8,9]. The thermal technique is useful to exhibit the distributions of fractions in solid samples by following their thermal behaviors [10].

On the other hand, although X-ray diffraction is not a preferred method for structural investigation of asphaltene [11], it was applied to asphaltene fractions but never to deposit or sediment samples till now.

The results of this study as well as other previous results [1,12,13] allowed us to elucidate the contribution of organic and mineral compounds in the formation of solid deposits.

2. Experimental

Three solid deposits were collected from three Mexican wells: K101, CH2 and T101 as well as samples of crude oils from the same wells. Each deposit was washed with toluene within a soxhlet unit, according to ASTM D 473 in order to separate the toluene-insoluble fraction, identified as deposit-residues. The deposit-asphaltenes were prepared by *n*-heptane precipitation from the toluene-soluble fraction according to ASTM D 4124.

The oil-sediments were obtained by centrifugation of crude oils for 30 min at 2000 rpm, while the oil-asphaltenes were precipitated from the sediment-free crude oils with *n*-pentane, following the ASTM D-2007 procedure.

The quantitative analysis was accomplished with an Elemental Vario EL apparatus, to obtain the carbon, hydrogen and nitrogen content, and a Leco SC-444 apparatus for sulfur content, while oxygen was calculated to obtain the 100 wt% of mass balance. Additionally, elements such as Fe, Ni, V, Ca, Mg, Al, Si, Na and Ba were quantified by using a Perkin–Elmer-5000 atomic absorption spectrophotometer (AAS). A Siemens D 500 diffractometer was used to obtain the diffraction patterns (XRD) of all samples. As the oil-sediment samples are paste-like, an aluminum sample holder was used for the measurement of their diffraction patterns [14]. The organic composition of all samples was studied by infrared spectroscopy in a Brucker EQUINOX-55 spectrometer (FTIR). The solid samples were prepared in KBr pressed disks, while the sediments were prepared as a film between two KBr windows. The thermal behaviors (TGA/DTG) of the deposit and sediment samples were determined according to ASTM Standard E 1131 procedure, in a Perkin–Elmer TGA-7 apparatus. The samples were burnt under air atmosphere from room temperature to 900 °C, at a rate of 10 °C min^{-1}.

3. Results

Each of the K101, CH2 and T101 wells is producing from the upper Jurassic Kimmeridge age zone reservoirs. Their location and depth as well as the crude oils characteristics as API gravity and asphaltene contents are presented in Table 1. These wells experience the effects of deposit formation 8–10 months after each cleaning process.

3.1. Samples composition

The K101 and CH2 deposits are black solids with brittle texture, while the T101 deposit is a black–gray semi-solid with a thick or gum-like texture. The K101, CH2 and T101 deposits contain 33.62, 5.55 and 6.99 wt% of toluene insoluble fraction identified as deposit-residue and 36.3, 74.46 and 42.19 wt% of *n*-heptane insoluble fraction, as deposit-asphaltene.

All the tested crude oils contain approximately 1:30 vol/vol of sediments, whereas the amount of asphaltene separated from K101, CH2 and T101 sediment-free oils are 3.1, 2.5 and 8.5 wt%, respectively. The elemental compositions of the deposits, oil-sediments and asphaltenes are presented in Table 2. The hydrogen content is similar in each deposit and their respective oil-asphaltene fraction. Therefore, their atomic ratios H/C are equal or slightly

Table 2
Elemental composition of deposits, asphaltenes and oil-sediments (wt%)

Elements	K101 well			CH2 well			T101 well		
	Deposit	Sediment	Oil-asphaltene	Deposit	Sediment	Oil-asphaltene	Deposit	Sediment	Oil-asphaltene
Weight (%)									
Carbon	83.66	85.71	85.70	82.61	85.08	86.61	80.29	85.50	87.20
Hydrogen	8.11	12.68	8.30	7.14	12.68	7.20	7.77	12.29	7.70
Nitrogen	0.86	0.14	1.00	0.71	0.09	0.56	0.63	0.19	0.86
Oxygen	2.54	0.10	1.37	0.51	0.24	2.94	5.03	0.13	1.14
Sulfur	3.39	1.37	3.63	6.19	1.90	2.69	5.22	1.89	3.10
Metals	1.44	0.003	0.001	2.84	0.004	0.0018	1.06	0.002	0.001
H/C atomic ratio	1.16	1.77	1.16	1.04	1.79	1.00	1.16	1.73	1.06

Table 3
Elemental composition of K101, CH2 and T101 deposits by atomic absorption spectroscopy (wt%)

	Fe	Ba	Si	Ca	Na	Ni	V	Al	Mg	K
K101	0.07	0.56	0.20	0.14	0.27	0.02	0.05	0.05	0.04	0.04
CH2	2.29	0.10	0.07	0.14	0.09	0.01	0.07	0.01	0.02	0.01
T101	0.17	0.38	0.19	0.08	0.13	0.01	0.04	0.03	0.02	0.01

greater. However, the carbon content of the oil-asphaltene is higher than the upper limit reported by Speight [15].

All deposits contain appreciable amounts of metals as shown in Table 3. The K101 deposit contains the highest amount of barium, sodium, silicon and calcium, 0.56, 0.27, 0.20 and 0.14 wt%, respectively. The CH2 deposit exhibits the highest amount of iron and vanadium, 2.29 and 0.07 wt%, respectively, while the T101 deposit contains only small amounts of these metals. On the contrary, the sediments and oil-asphaltenes contain much fewer metals compared to deposit composition, although Na, V, Ca and Al were found as the outstanding elements in these samples. However, in the deposit compositions, the content of vanadium and nickel has no proportion with the amounts of these metals in the oil-asphaltenes.

3.2. X-ray diffraction

Crystalline compounds were identified by XRD in oil-sediments (Fig. 1) and deposit-residues (Fig. 2). Barite (JCPDS 76-0214), calcite (JCPDS 05-0586), quartz (JCPDS 05-0490) and halite or NaCl (JCPDS 01-0993) were identified in the oil-sediment diffractograms. The K101 deposit-residue diffractogram contains barite, calcite, aragonite (JCPDS 03-0893), dolomite (JCPDS 79-1346), quartz and halite. The CH2 deposit-residue diffractogram contains the same compounds but also iron compounds as goetite (JCPDS 02-0273), lepidocrocite (JCPDS 02-0127), magnetite (JCPDS 11-0614) and pyrrhotite (JCPDS 13-1028). Finally, the T101 deposit-residue contains barite, calcite, aragonite halite, quartz, dolomite and also hidrobiotite (JCPDS 13-0233).

Calcite and aragonite are calcium carbonates and they are considered crude oil endogenous materials as quartz, halite, dolomite and hidrobiotite. Halite or sodium chloride, which is part of the reservoir brine, is a steel aggressive corrosion agent. Additionally, barium sulfate ($BaSO_4$) is still used as drilling mud component, and therefore, its presence explains the high amount of sulfur of the deposits.

On the other hand, amorphous structures prevail in the deposits, deposit-asphaltene, oil-asphaltene and sediments

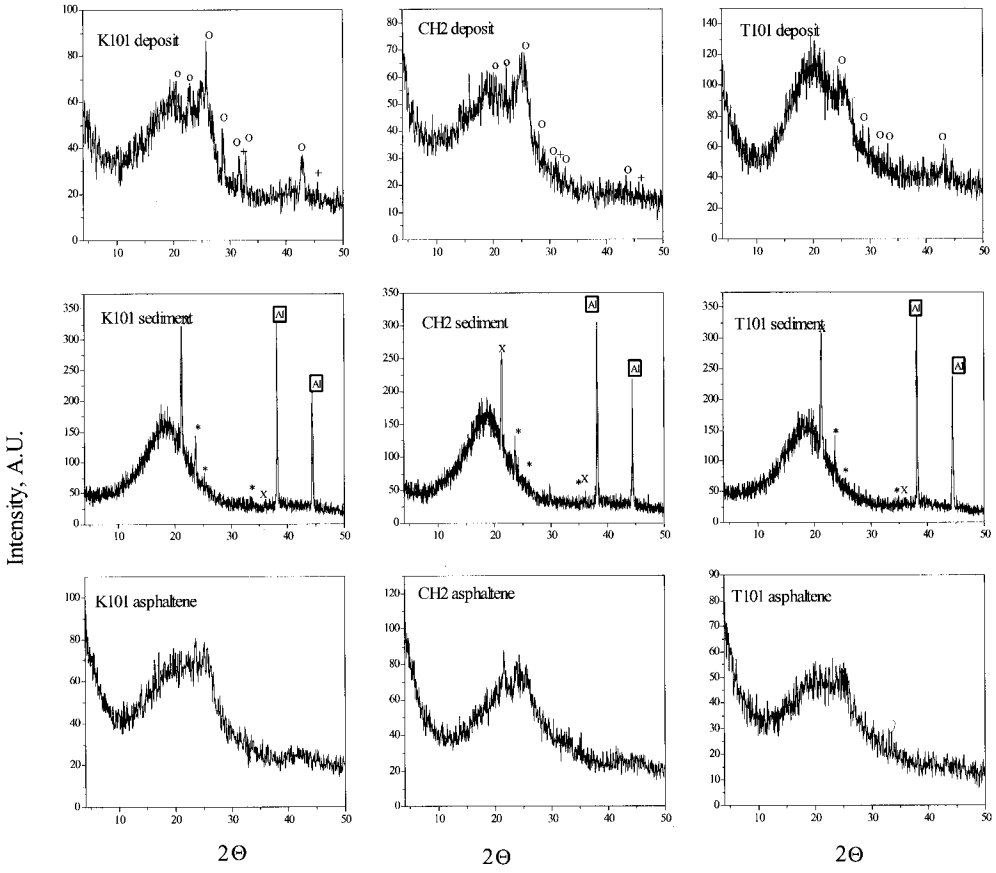

Fig. 1. X-ray diffraction patterns of the deposits, oil-sediments and asphaltenes. Symbols: (O) $BaSO_4$; (*) dolomite; (x) SiO_2; (+) NaCl and Al signal corresponds to the sample holder.

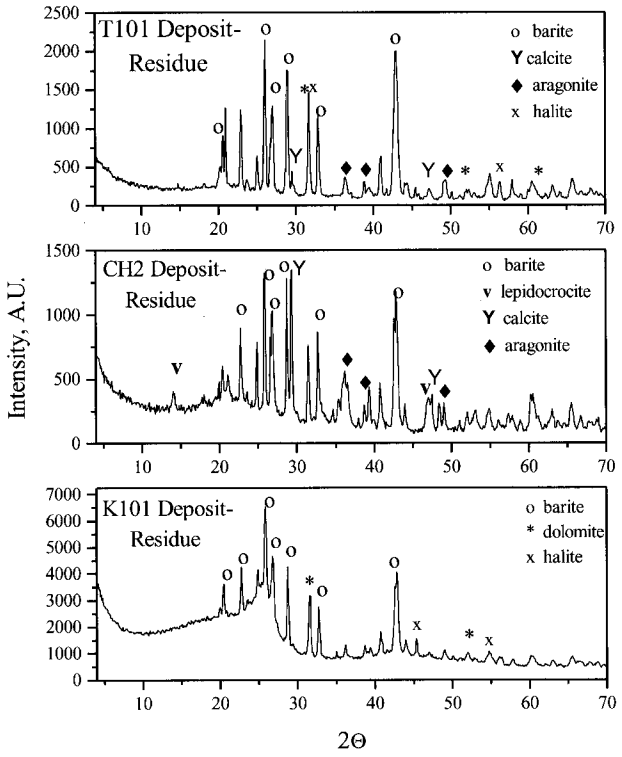

Fig. 2. X-ray diffraction patterns of the deposit-residues, including some compounds identification.

as their XRD patterns shown. Furthermore, a careful observation of the base line of the deposit and oil-asphaltene diffractograms in Fig. 1 reveals two wide bands rising at 20 and 25° (2θ), which correspond to γ and (002) bands [8], respectively. The packing distance between saturated structures aliphatic chains or naphtenic rings originates the γ band, while the (002) band represents the spacing between stacked aromatic layers or graphite layers [8]. The selected band areas were measured at reduced intensity (background subtracted) by means of the PROFILE V 1.4 of the DIFFRAC-AT V3-1993 program from SIEMENS, applying Lorentz function as the fitting function. The structural parameters of the deposit, deposit-asphaltene, oil-asphaltene and sediments were calculated according to the literature [8,16] and presented in Table 4. Thus, the aromaticity factors calculated as the ratio of the (002) area and the sum of (002) and (γ) areas [8] reveal that the aromaticity of both oil- and deposit-asphaltenes is larger than the deposits. No aromaticity factors were calculated for the sediments, as the (002) band was not observed in their diffractograms. The mean crystallite diameters corresponding to the (002) and (γ) bands were calculated on the basis of the Debye-Scherrer crystallite size formula [16] using graphite size parameters for the correction factor. The crystallites average diameter indicates how amorphous the sample is: a low crystallite size indicates a high amorphous sample, while a high crystallite size is related to some crystallization degree.

All deposits registered the lowest values of the average diameters for the saturated portion of the molecules ϕ_γ,

Table 4
Crystallite parameters calculated from X-ray diffractograms (Φ_γ,$\gamma\Phi_{002}$ are the diameters of crystallites, Å calculated on basis of the Debye–Scherrer formula. d_m is the layer distance between aromatic sheets and d_γ is the interchains layer distance in the saturated portions of the molecules. FWHM is the full width at half-maximum high of the band)

Parameters	K101 deposit	K101 deposit-asphaltene	K101 oil-asphaltene	K101 sediment	CH2 deposit	CH2 deposit-asphaltene	CH2 oil-asphaltene	CH2 sediment	T101 deposit	T101 deposit-asphaltene	T101 oil-asphaltene	T101 sediment
(γ) band position, 2θ	19.54	20.32	19.96	18.25	19.53	19.68	19.744	18.3	19.84	20.04	18.34	18.82
											21	
FWHM of (γ) band	7.23	2.78	3.59	8.016	9.62	5.87	2.53	7.68	10.72	9.16	2.72	9.75
											3.61	
(002) band position, 2θ	25.18	25.02	24.70		25.52	25.09	24.37		25.64	25.46	24.76	
FWHM of (002) band	3.30	3.70	2.73		2.28	5.67	5.52		2.75	3.88	4.02	
f_a	0.30	0.76	0.45		0.20	0.75	0.87		0.09	0.36	0.52	
d_m (Å)	1.81	2.28	2.30		1.81	1.82	1.87		1.78	1.79	1.84	
d_γ (Å)	2.88	2.21	2.56	3.07	2.88	2.86	2.85	3.06	2.84	2.81	3.06	1.94
											2.68	
Φ_γ (Å)	71.9	169.1	132.20	49.37	37.2	86.2	177.2	69.55	29.85	45.6	170.15	34.2
											132.15	
Φ_{002} (Å)	143.3	132.0	170.18		190.15	91.05	95.9		171.9	123	120.3	

while the largest values were calculated for the CH2 and T101 oil-asphaltenes and for K101 deposit-asphaltene. Moreover, in the T101 oil-asphaltene, the γ peak was found to be double, at 18.34 and 21° (2θ), which indicates the presence of two types of saturated structures. On the other hand, all deposit-asphaltenes exhibit the lowest value of the average diameters for the aromatic sheets ϕ_{002}, while the largest values were calculated for the CH2 and T101deposits as well as for K101 oil-asphaltene.

3.3. Fourier transform infrared spectroscopy

The infrared spectra of the deposit, oil-asphaltene and sediments presented in Fig. 3 are dominated by the vibration bands characteristic of CH_2 and CH_3 groups with no significant shifts of these vibrations from their normal positions [17]. The main differences between these spectra are related to the relative intensities of the stretching vibration modes of the methyl and methylene groups, as well as to their skeletal vibrations at low frequencies. By comparing the ratios of the intensities of ν-CH_2 out-of-phase and in-phase vibrations at 2920 and 2850 cm^{-1}, respectively, we found that the deposits contain more in-phase methylene group vibration than asphaltenes and oil-sediments. Additionally, the δ-CH_2 vibration band moves at a lower frequency (approximately 1453 cm^{-1}) in all deposits as well as in the CH2 oil-asphaltene spectrum. This is possible only if these vibrations are inhibited by a special orientation of hydrocarbon chains in solid phase or in cyclic structures. This band conserves its normal position at 1460 cm^{-1}, in the spectra of the other samples. A doublet, sharp and well-defined, was clearly observed in the T101 sediment spectrum in the 720–750 cm^{-1} region, corresponding to methylene wagging band of solids straight-chain hydrocarbons at room temperature [18], which means that this sediment is composed mainly by paraffin waxes.

Each spectrum exhibits a band at 1600 cm^{-1}, which corresponds to aromatic skeletal ring breathing vibration with small shoulders between 1600 and 1500 cm^{-1}. However, in the T101 deposit, the band at 1614 cm^{-1}

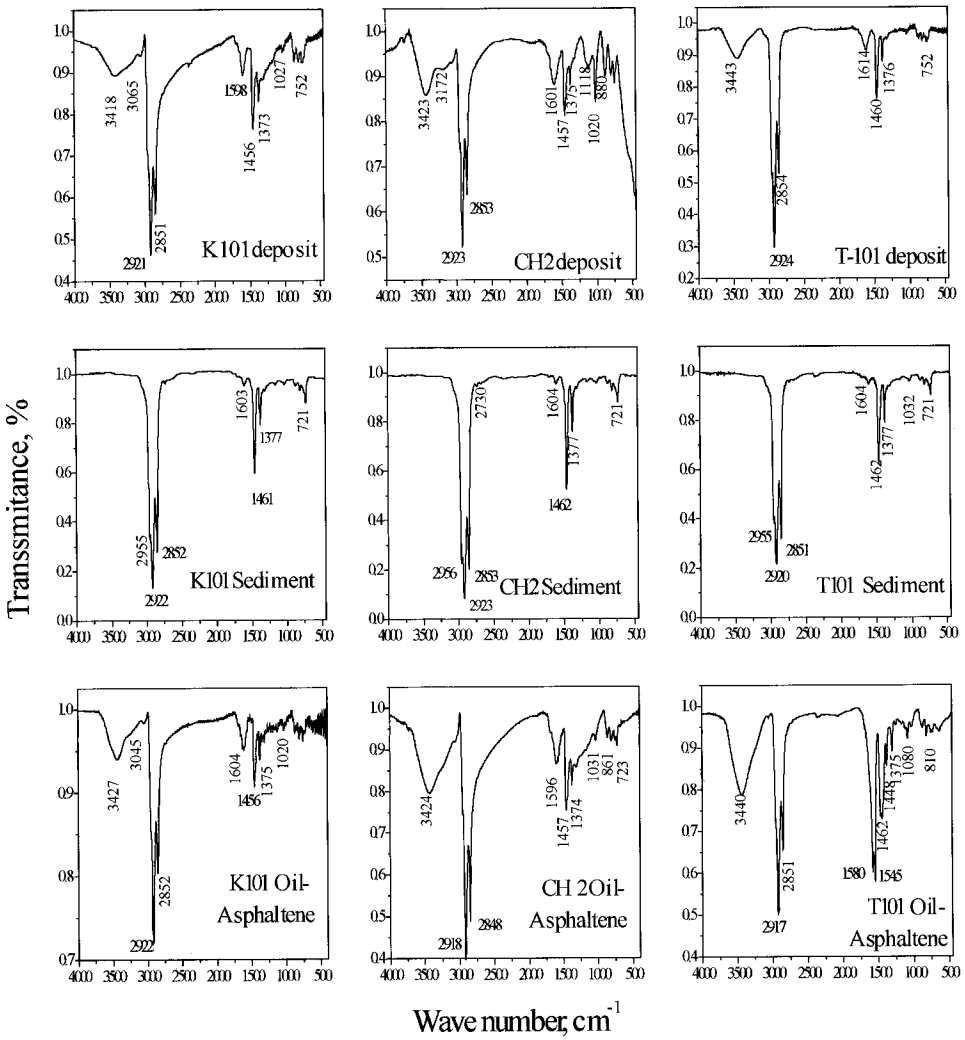

Fig. 3. FTIR spectra of the deposits, oil-sediments and asphaltenes.

indicates the presence of adsorbed water rather than aromatic rings. On the other hand, the presence of stretching and deformation vibration bands at 3040 and 1410 cm^{-1} corresponding to C=C double bonds are only evident in the K101 and CH2 oil-asphaltenes and deposits.

The wide band observed from 3550 to 3100 cm^{-1}, in the deposits and oil-asphaltenes spectra corresponds to hydroxyl groups stretching vibrations of water molecules adsorbed between mineral layers, rather than to hydroxyl organic compounds [19]. Moreover, this band could hide the stretching vibration modes of N–H bond, as in the case of T101 oil-asphaltene, which shows the presence of secondary non-cyclic amides [18] by the sequence of bands at 1580 and 1546 cm^{-1}. A wide shoulder extended from 2800 to 2500 cm^{-1} was observed in the K101 and CH2 deposits and CH2 oil-asphaltene spectra. This band is normally found in each asphaltene spectra and was attributed to hydrogen bonds [20,21], although the enolic form of ketone compounds as well as some amine salts exhibit bands in this range [18].

Identification by FTIR of inorganic compounds is difficult in the organic samples. Therefore, such compounds were well identified by FTIR in the CH2 and T101 deposit-residues, while the K101 deposit-residue spectrum still preserves bands corresponding to organic compounds, as shown in Fig. 4. However, in this last sample, the vibration bands corresponding to aromatic as well as polyaromatic compounds are enhanced.

On the contrary, the CH2 deposit-residue spectrum is dominated by strong vibration bands of carbonate at 1423 and 875 cm^{-1}, sulfate at 1086 and 601 cm^{-1}, as well as silicate compounds at 981 cm^{-1}. Additionally, small vibration bands corresponding to iron hydroxide and iron oxide were detected in the low frequencies region of this spectrum [22]. Finally, the T101 deposit-residue spectrum shows strong bands corresponding to sulfate at 1086 and 609 cm^{-1} as well as small bands of carbonate and silicate compounds.

Differences between deposit and deposit-asphaltene spectra (not shown) are minimal. The intensities of the methyl and methylene vibration bands are reduced in the deposit-asphaltene spectra, and the deformation vibration bands are slightly shifted from their normal position and the methyl and methylene asymmetric bending vibration bands are clearly separated. Additionally, the aromatic rings out of plane deformation vibration bands are intensified in the deposit-asphaltene spectra, which agree with the XRD results. The deposit-asphaltene spectra also exhibit bands corresponding to the C=O and C=C bonds stretching vibration probably in ketones and other unsaturated compounds, respectively.

3.4. Thermal behavior

The TG first derivative profile (DTG) is a sequence of defined peaks, which are associated to the amount of weight loss during each thermal event. For example, Bermejo [10] identified in the asphaltene DTG profile only one peak rising between 400 and 500 °C. Thereby, it is assumed that this peak could be assigned positively to asphaltene in each DTG profiles of the deposits and oil-sediments. TG analysis of deposits and the oil-sediments are summarized in Tables 5–7 and the corresponding DTG profiles are shown in Fig. 5. The DTG profile of oil-sediments exhibits four well-defined peaks, while the profile of deposits shows three main peaks. The first peak emerging around 100 °C represents 37–65 wt% of the initial weight in the T101 deposit and all the sediments. None of the DTG profiles of the other deposits exhibit this peak, as it corresponds to water or low-molecular weight hydrocarbons. The second peak, between 300 and 400 °C, which represents 13–30 wt% of the initial weight of the oil-sediment samples, is also missing in the DTG profile of the deposits. The third peak, between 400 and 500 °C, which corresponds to asphaltene fraction [10], was observed in all sample profiles, although the K101 deposit profile exhibits two peaks instead of one. The amount of weight loss represented by this peak is 13–20 wt% in the deposits and 8.5–12.5 wt% in the oil-sediments. The shape of the peak emerging beyond 500 °C in the DTG profiles of the samples is different in the deposits than in the sediments and it represents minerals and heavy-molecular weight hydrocarbons. Thus, in the K101 deposit the peak is wider compared to the oil-sediment corresponding peak. In the CH2 deposit, the peak is wider than in its corresponding sediment and it moves to a higher temperature. On the contrary, in the T101 deposit, this peak is higher than in the oil-sediment and it moves down to a minor temperature. The combustion of the deposits left a higher amount of ash (2.8–4.4 wt%) than the sediments (less than 1 wt%). However, the amount of the deposit-ashes is inferior compared to the deposit-residue obtained by extraction with toluene.

4. Discussion

Two solid deposits (K101 and CH2) and a semi-solid deposit (T101), their asphaltene and residues, as well as the oil-asphaltene and oil-sediment fractions separated from the corresponding crude oils were characterized.

Deposits contain less carbon than the oil-asphaltene, while their hydrogen content is similar to the T101 deposit, or inferior as the two other deposits, but their H/C atomic ratios are similar. However, both aromaticity factors and structural parameters calculated from their diffractograms are distinct. Thus, the deposit aromaticity factors are lower than those of the oil-asphaltenes and deposit-asphaltenes. Furthermore, the average diameters of the saturated portions of molecules of the deposits are low as an indication of small saturate structures. This part corresponds to *n*-heptane-soluble portion of the deposit, which contributes to the aromaticity factors reduction. On the contrary, the deposit average diameters of the aromatic crystallites are larger compared to those calculated for oil-asphaltene and even for the deposit-asphaltenes. Moreover,

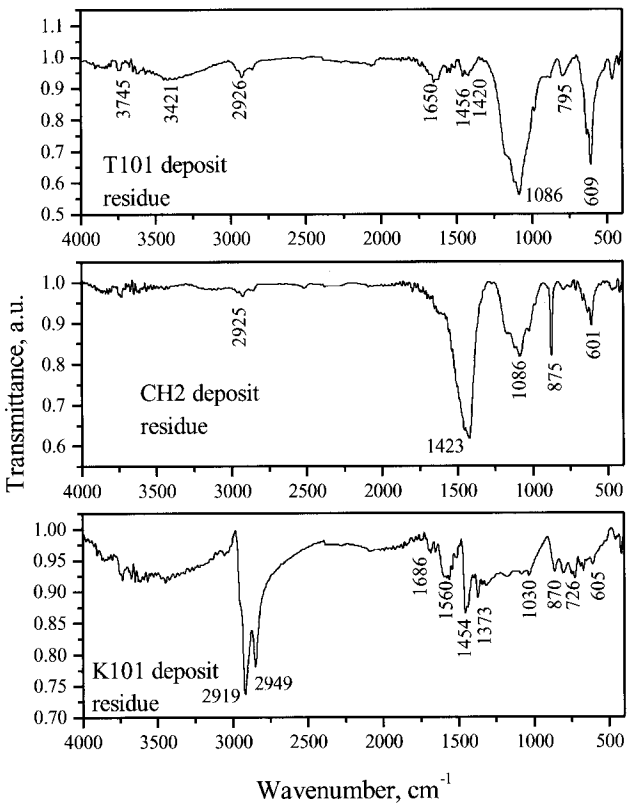

Fig. 4. FTIR spectra of the deposit-residues.

the difference between the average diameters of the aromatic sheets ϕ_{002}, calculated for the deposit and deposit-asphaltenes indicates that the solvents induced the disruption of the aromatic sheet crystalline organization reached in the deposits. These results agree with literature indication on the different nature of asphaltene obtained in laboratory by solvent precipitation and those induced by pressure depletion inside the petroleum well [4].

Additionally, these results also suggest that the deposit H/C atomic ratios must be lower than those of oil-asphaltene, which means that part of the deposit-carbon must originate by calcite or aragonite ($CaCO_3$) combustion. Indeed, FTIR and XRD showed the presence of such carbonate minerals in the deposit-residues, as they are related to the sedimentary rocks of the reservoirs. Moreover, barite ($BaSO_4$) could be the source of the high amount of sulfur detected in the CH2 and T101 deposits.

On the other hand, iron, which was found in a higher amount in the CH2 deposit elemental composition, was identified by XRD as iron oxide, hydroxide and sulfide compounds. Thus, while iron hydroxides as well as halite (NaCl) indicates moisture or brine wetting the tubing surface, iron sulfides as pyrrhotite ($Fe_{1-x}S$) also point out a corrosion process in the presence of sulfur bearing compounds. Indeed, such compounds are generally formed in situ on the carbon–steel tubing surface as a consequence of reaction with sulfur compounds as H_2S [23,24]. Pyrrhotite was previously identified along with maghemite, which is also a non-stoichiometric iron compound, on the surface of a tubing piece collected from the CH2 well [13]. Such iron non-stoichiometric compounds represent the active phases of iron-containing catalysts, which are used in hydrogen and oxygen interchange processes [25] or in carbon–carbon bond scission [26]. Consequently, the presence of iron compounds within the deposit compositions indicates that the tubing scale layer compounds are involved in the deposit constitution together with the other minerals, as iron sulfide and oxyhydroxyde crystals. Moreover, the identification of polar compounds in the deposit-asphaltene spectra, but not well detected in the oil-asphaltene spectra, agrees with reported results [6] on the increasing of the polar fraction content of the oil *n*-heptane precipitated fraction as a consequence of the Fe ion presence.

The amount of deposit-asphaltene fraction, quantified from the 400–500 °C DTA weight loss peak is about three times lower than the amount of asphaltene fractions obtained by precipitation with *n*-heptane from the deposits. At the same time, the huge amount of material loss beyond 500 °C must also correspond to the *n*-heptane insoluble fraction. These results also agree with the values of high aromaticity factors calculated from the XRD diffractograms of the deposit-asphaltene fractions, which point out the presence of polyaromatic compounds.

Additionally, the deposit thermal behavior could be

Table 5
TG analysis of K101 deposit and oil-sediment

Fractions eliminated	K101 deposit		K101 sediment	
	Temperature interval (°C)	Weight loss (wt%)	Temperature interval (°C)	Weight loss (wt%)
Low-molecular weight fraction			26–266	51.67
	30–325	26.81	266–413	29.75
	325–360	1.50	–	–
Asphaltene fraction	360–434	7.06	–	–
	434–478	6.36	413–500	8.46
High-molecular fraction and minerals	478–625	23.35	500–636	9.65
	625–833	30.55	–	–
Ash	–	4.37	–	0.47

Table 6
TG analysis of CH2 deposit and sediment

Fractions eliminated	CH2 solid deposit		CH2 sediment	
	Temperature interval (°C)	Weight loss (wt%)	Temperature interval (°C)	Weight loss (wt%)
Low-molecular weight fraction	–	–	26–281	65.53
	26–352	16.26	281–370	15.83
Asphaltene fraction	–	–	370–390	0.71
	352–509	20.53	390–486	7.74
High-molecular fraction and minerals	–	–	486–590	10.06
	509–770	60.41	–	–
Ash		2.80		0.13

Table 7
TG analysis of T101 deposit and sediment

Fractions eliminated	T101 semi-solid deposit		T101 sediment	
	Temperature interval (°C)	Weight loss (wt%)	Temperature interval (°C)	Weight loss (wt%)
Low-molecular weight fraction	–	–	26–202	37.38
	27–105	15.76	–	–
	105–310	40.20	202–265	13.54
	351–395	1.90	265–394	24.72
Asphaltene fraction	–	–	394–416	1.86
	395–487	12.91	416–433	1.92
			433–501	8.57
High-molecular fraction and minerals	487–620	25.46	501–807	11.97
Ash		3.77		0.04

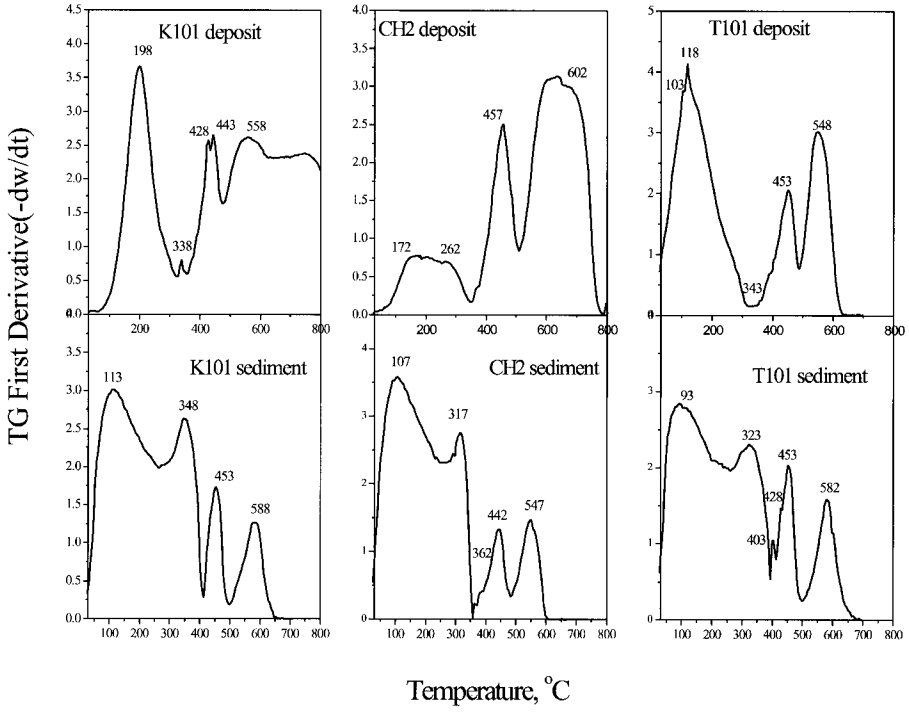

Fig. 5. DTG profiles of the deposits and oil-sediments.

explained by the presence of minerals in their composition. Some of these minerals can act as adsorbents of organic molecules, and consequently, they may delay the deposits combustion [5] or the extraction process. This could be the meaning of the high amount of deposit-residue obtained by toluene extraction, while the low amount of deposit-ash indicates that the deposit experienced the decomposition of most of the minerals as carbonate and sulfate, during the thermal procedure.

On the other hand, nickel and vanadium are referred as porphyrin complexes partitioned between asphaltene and resin fractions. At the time of precipitation, the vanadyl porphyrins may be strongly adsorbed or bonded to asphaltene via V–O or V–N bonds [27]. These metals were found in all deposits in a higher amount than in the corresponding oil-asphaltenes or sediments. Consequently, since inorganic vanadium compounds were not clearly detected in the deposits by the applied methods or on the CH2 tubing surface examined elsewhere [12], they must exist in organic structures as porphyrins, associated to the organic part of the deposits. Furthermore, their abundance in the deposits indicates a time-dependent process of accumulation by their selective adsorption from petroleum flow on the surface of metal or on mineral particles.

5. Conclusions

The main chemical and structural differences between deposits and oil-asphaltene are related to the saturated and aromatic contents. Indeed, neither the deposit nor deposit-asphaltene exhibits structural or compositional concordance with oil-asphaltene. Moreover, all deposits contain a high amount of minerals carried out from the reservoir as calcite, aragonite, halite and quartz, from the drilling mud constituents as barite as well as from steel corrosion as iron hydroxides and sulfides formed in situ on the tubing surface. Furthermore, as vanadium and nickel are related to the petroleum organometallic compounds, their high amounts in the deposits indicate an unperturbed time-depending process of accumulation of such compounds on the tubing surface along with high-condensed aromatic systems.

Acknowledgements

This research was supported by Instituto Mexicano del Petroleo, Grand FIES 97-06-I. The authors are thankful to Dr H. Yee-Madeira (ESFM-IPN, Mexico) for providing the FTIR facilities.

References

[1] Cosultchi A, Garcíafigueroa E, García-Borquez A. 14th International Congress on Electron Microscopy, Cancun, Mexico. August 31–September 4, 1998.
[2] Carbognani L. Vision Tecnol 1995;3(1):35.
[3] Koots JA, Speight JG. Fuel 1975;54:179.
[4] Joshi NB, Mullins OC, Jamaluddin A, Creek J, McFadden J. Energy Fuel 2001;15:979–86.
[5] Bishop AN, Philp RP. Energy Fuel 1994;8:1494–7.
[6] Nalwaya V, Veerapat T, Pornpote P, Scott F. Ind Engng Chem Res 1999;38:964–72.
[7] Piro G, Canonico LB, Galbariggi G, Bertero L, Carniani C. SPE production & facilities. August 1996. p. 156–60.
[8] Schwager I, Farmanian PA, Kwan JT, Weinberg VA, Yen TF. Anal Chem 1983;55:42–5.
[9] Tartarelli R, Giorgini M, Getti P, Belli R. Fuel 1987;66(10):1737.
[10] Bermejo J, Granda M, Menendez R, Garcia R, Tascon JMD. Fuel 1997;76(2):79.
[11] Barman BN, Skalos L, Kushner DJ. Energy Fuel 1997;11:593–5.
[12] Cosultchi A, Garciafigueroa E, Muñoz A, Zeifert B, Garcia-Borquez A, Lara VH, Bosch P. Surf Rev Lett 1999;6(6):1299.
[13] Cosultchi A, Garciafigueroa E, García-Bórquez A, Reguera E, Yee-Madeira H, Lara VH, Bosch P. Fuel 2001;80(13):1963–8.
[14] Lara VH, Bosch P. Rev Inst Mexicano Petroleo 1992;XXIV(4):50–5.
[15] Speight JG. ACS Adv Chem Ser No 195 1981:1–15.
[16] Bonetto RD, Viturro HR, Alvarez AG. J Appl Cryst 1990;23:1136–7.
[17] Bellamy LJ. The infrared spectra of complex molecules. 3rd ed, vol. 1. New York: Chapman & Hall, 1975.
[18] Socrates G. Infrared characteristic group frequencies. 2nd ed. Chichester, England: Wiley, 1997.
[19] Famer VC. Mineralogical society. Monograph 4. The infrared spectra of minerals. London: Mineralogical Society, 1974.
[20] Speight JG. Appl Spectrosc Rev 1994;29:269–307.
[21] Ignasiak T, Strausz OP, Montgomery DS. Fuel 1977;56(10):359.
[22] Raman A, Kuban B, Razvan A. Corros Sci 1991;32(12):1295–306.
[23] Narayanacharyulu PBV. Early stages of sulfidation of iron and iron-chromium alloy in hydrogen sulfide. PhD Thesis. Iowa State University, Ames, IA, 1982.
[24] Favre M, Landolt D, Hoffman K, Stratmann M. Corros Sci 1998;40(4–5):493.
[25] Kung HH. Transition oxide metal: surface chemistry and catalysis. Studies in surface science and catalysis, vol. 45. Amsterdam: Elsevier Scientific, 1989.
[26] Linehan JC, Matson DW, Darab JG. Energy Fuel 1994;8:56–62.
[27] Filby RH, Strong D. Tar sand and oil upgrading technology, AICHE Symposium Series, 282(87). New York: AICHE, 1991. p. 1–9.